Journal of Mines, Metals and Fuels, *71(11): 1906-1918; 2023. DOI: 10.18311/jmmf/2023/35156*

Print ISSN : 0022-2755

Journal of Mines, Metals and Fuels

Contents available at: *www.informaticsjournals.com/index.php/jmmf*

Investigation of Mechanical and Wear Behaviour of Al5056-Carbon Nanotube -Graphene Hybrid MMCs using Powder Metallurgy Route

Nagaraja C. Reddy[1]*, B. M. Girish[2], B. M. Satish[3], Mahesh B. Davanagere[4], L. Girisha[5], E. R. Babu[1] and Chithirai Pon Selvan[6]

[1]Department of Mechanical Engineering, Bangalore Institute of Technology, Bengaluru - 560004, Karnataka, India; cnraaja@gmail.com

[2]Department of Mechanical Engineering, Alliance College of Engineering and Design, Alliance University, Bangalore - 562106, Karnataka, India

[3]School of Engineering, Mohan Babu University, Tirupati - 517102, Andhra Pradesh, India

[4]Department of Mechanical Engineering, Graphic Era (Deemed to be University), Dehradun -248002, Uttarakhand, India

[5]Department of Mechanical Engineering, PES Institute of Technology and Management, Shivamogga - 577204, Karnataka, India

[6]School of Science and Engineering, Curtin University, Dubai - 345031, United Arab Emirates

Abstract

Composites containing metal at least in two constituent parts are metal matrix composites. Another material may also be used like organic compounds or ceramics, in addition to a different metal. In the current work Al5056 aluminium powder is used as the matrix material having an average particle size was about 35±5 µm and Carbon Nanotube (CNT) and Graphene (Gr) are used as reinforcement materials. Hybrid composites are developed using an advanced powder metallurgy technique process. Also, in the existing work microstructure characterization was performed using advanced techniques. Hardness, Tensile and wear tests are conducted as per ASTM standards. Mechanical properties improved with the increase in amalgams in the matrix. The wear surface morphology of Al alloy shows a rough surface with more grooves and ridges compared to the wear surface morphology of Al5056/CNT-Gr hybrid composites. Wear debris results of Al alloy show more debris chips out of the material compared to Al5056/CNT-Gr hybrid composites.

Keywords: *Al5056-Alloy, CNT, Gr, Hardness, Microstructure, Tensile, Wear*

1.0 Introduction

Composites containing metal at least in two constituent parts are metal matrix composites. Another material may also be used like organic compounds or ceramics, in addition to a different metal. Compositions that are composites have generally better properties compared to an independent or a single component. Reinforcing materials are dispersed in a metal matrix (typically ductile) to create MMCs[1]. It is possible to coat the reinforcement surface so that a reaction of chemicals would not take place with the matrix. In a matrix, the

*Author for correspondence

reinforcement is embedded in a completely continuous monocrystalline or monolithic single-crystal material. It implies that, unlike two sandwiched materials, there's a way in the material to any direction through the matrix. Within the matrix, the reinforcement is incorporated[2]. Reinforcing a compound not only assists with structural purposes, but reinforcement also delivers in enhancing the properties of the compound in terms of, for example, corrosion resistance, friction coefficient, lightweight, corrosion resistance, and high ability to conduct heat. Both discontinuous and discontinuous reinforcing are possible. The properties of these alloys can be tailored to be exceptional to those of monolithic alloys, such as thermal fatigue resistance, stiffness, heat resistance and wear resistance by adding reinforcements such as ceramics SiC, B_4C etc[3-5]. In discontinuous MMCs, whiskers or coarse fibres often provide the reinforcement, and are vulnerable to cracking owing to the brittle reinforcement existence, such as in Al/SiC or Al_2O_3 composites, and cannot be worked with standard metalworking techniques like rolling and forging extrusion. MMCs are widely used in a variety of applications due to their unique characteristics, which include superior stiffness, wear resistance and service temperatures, including a brake rotor, cylinder liners, automobile drive shaft, and connecting rod[6]. Metal Matrix Composites (MMCs) offer a range of physical and mechanical properties which make them highly desirable aspirant materials for use in the automotive sector, the aerospace sector and other fields[7]. Recent attention has been devoted to particulate-reinforced MMCs due to their comparatively inexpensive cost and isotropic characteristics.

Compared to monolithic alloys, the MMCs possess numerous benefits like stiffness, enhanced wear and creep resistance, elastic modulus, low density, greater strength-to-weight ratio, and high specific strength[8]. As a result of their high manufacturing costs, MMCs have had limited application over the last few decades. However, the development of fly ash-reinforced MMCs has facilitated the development of light and cost-effective components and machine parts for automotive, machine tools and other applications[9]. An important feature of the present work is the characterization of Al5056 hybrid-MMCs reinforced with CNT and Gr through powder metallurgy.

2.0 Materials and Methodology

The present work used Al5056 powder with a size of particle about 35±5 μm as a matrix material. Also, in the present work Carbon Nanotube (CNT) and graphene are used as reinforcement material. CNTs (Carbon Nanotubes) exhibit exceptional electrical and thermal conductivity, alongside remarkable mechanical properties. Known as potentially the most efficient electron field-emitters, these pure carbon polymers can be chemically altered using extensive and established carbon chemistry.

Graphene is renowned for its toughness, flexibility, lightweight nature, and high resistance. It is estimated to be 200 times stronger than steel and five times lighter than aluminium. These qualities make graphene a versatile material, finding applications in diverse sectors like energy, construction, healthcare, and electronics.

Composites are developed using advanced powder metallurgy techniques using a spark plasma sintering process.

Table 1. Designation of Al5056/CNT-Gr hybrid-composite

S/no	Alloy/Composite Label	Notation
1	Al5056 alloy	Als
2	Al5056 alloy, (0.5% CNT + 2%Gr:)	Al-0.5C-2G
3	Al5056 alloy, (0.5% CNT + 3%Gr:)	Al-0.5C-3G
4	Al5056 alloy, (0.5% CNT + 5%Gr:)	Al-0.5C-5G

Spark Plasma Sintering (SPS) is a modern method for fabricating high-quality materials. Here are a few key points summarizing the process: SPS is a swift method of sintering materials, typically taking only a few minutes. It utilizes a pulsed electric current to heat the material, aiding in efficient sintering. Concurrently, mechanical pressure is applied to compact the material, enhancing density. SPS often requires lower temperatures compared to conventional sintering techniques. The process enables better control over grain growth, resulting in finer microstructures. Suitable for a variety of materials, including ceramics, metals, and composites. Produces materials with high density and strong mechanical properties.

2.1 Fabrication of Specimens

Composites are developed using advanced powder metallurgy techniques using a spark plasma sintering process. Spark Plasma Sintering (SPS) is a stress-aided pulsated-flow method in which the powder pellets are stacked in an electrified conductive mould and sintered in a uniaxial intensity. Al 5056 powder was ball milled with Gr and CNTs at a speed of 300 rpm for 2 Hrs, sintered at 400°C temperature and compacted at 50 MPa applied pressure and samples were prepared as per ASTM standards.

2.2 Experimental Details and Methodology Flowchart

To sort of ray used to illuminate the item is the primary distinction between an optical (OM- Model: Nikon LV150) and scanning electron microscope (SEM-Model: TESCAN Vega 3 LMU). The hardness test is conducted using a Vickers hardness tester (Model: VH1150). Samples are polished neatly and kept under the table sample grid.

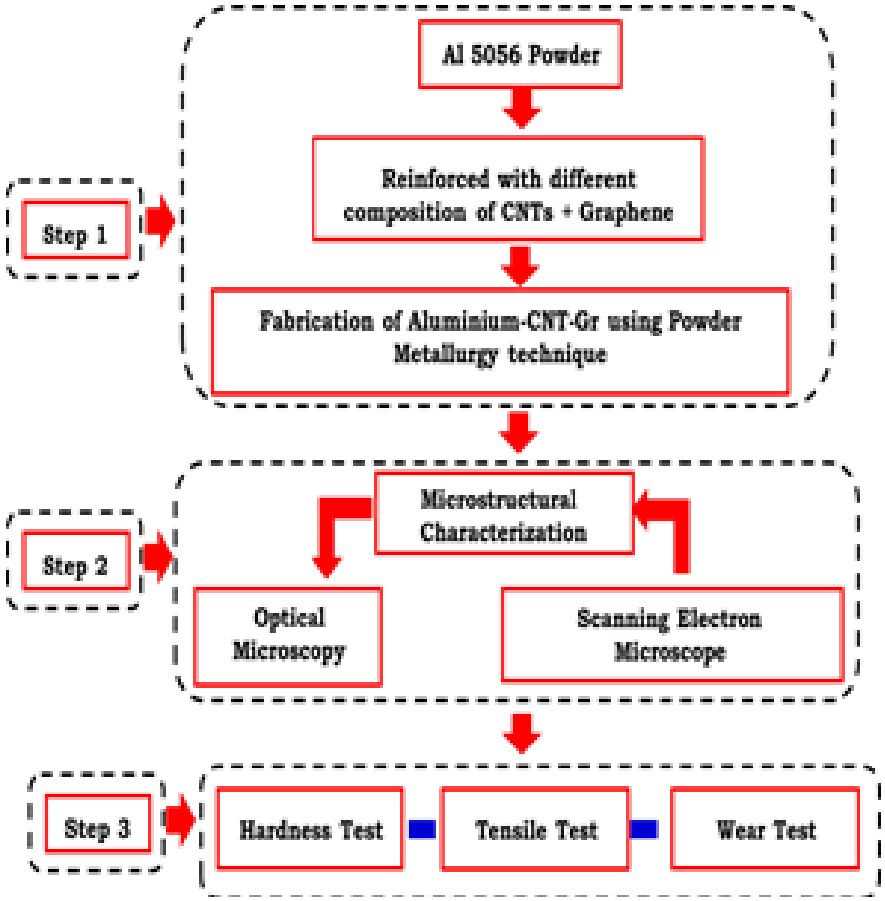

Figure 1. Methodology Flowchart.

A later sample is placed on a table grid and a load of 15 Kgf is applied for 15 seconds, and later analysed as per ASTM E384 standards are described in the monitor and displayed. The tensile test is done using UTM (Model: TUE-C-400). The sample is prepared as per ASTM E8M-15a standard. The specimen is clamped between two jaws of the testing machine and a strain rate of 2 mm/sec is applied on it. Wear parameters such as load, time as well and sliding speed are set and performed according to G99 standards. Later the wear-out samples are analyzed for wear track study using SEM.

3.0 Results and Discussions

This chapter explains the results and discussions of Al5056 alloy powder reinforced with B_4C using the powder metallurgy route.

3.1 Microstructure Analysis

3.1.1 Powder Morphology of CNT and Graphene using SEM

SEM micrograph of CNT and Graphene is shown in Figure 2 (a) and (b) respectively. Figure 2 (a) shows a yarn-like form with clusters of yarn at a few places. Also, CNT with high amplification has been illustrated which clearly shows the yarn form of CNT. Figure 2 (b) shows graphene clusters at a few places with irregular morphology. Also, graphene with high amplification has been illustrated. A few researchers have made similar observations[10,11].

3.1.2 Microstructural Characterization of Al5056/ CNT-Gr Hybrid-composites using OM

The Figure shows Optical Micrographs of Al 5056 alloy and its CNT/Gr hybrid composites. The 3 (a) depicts Al 5056 alloy OM, 3 (b) depicts OM of Al 5056 + (0.5% CNT + 2%Gr: Al-0.5C-2G) 3 (c) depicts OM of Al 5056 + (0.5% CNT + 3%Gr: Al-0.5C-3G) and 3 (d) depicts OM of Al 5056 + (0.5% CNT + 5%Gr: Al-0.5C-5G) its hybrid-composites. The microstructure plainly shows a genuinely uniform circulation of fortification (Gr + CNT) with negligible absorbency in the lattice amalgam in all the cast amalgamated frameworks considered. Microstructure comprises fine encourages in a framework of dendritic Aluminum strong arrangement. Isolation or porosity isn't found in the area. We can see the fair dispersal of the bolstering specks in the milieu. The murky district shows the milieu, and the silvery hue shows the dispersal of buttressing particles (Gr + CNT). It shows twitch particles area unit well spread uniformly within the Al matrix. This was attributed to the effective stirring action and use of acceptable stir-casting method parameters throughout the casting method. Typically, the rise in weight share of reinforcement in composites ends up in consistency problems[12,13].

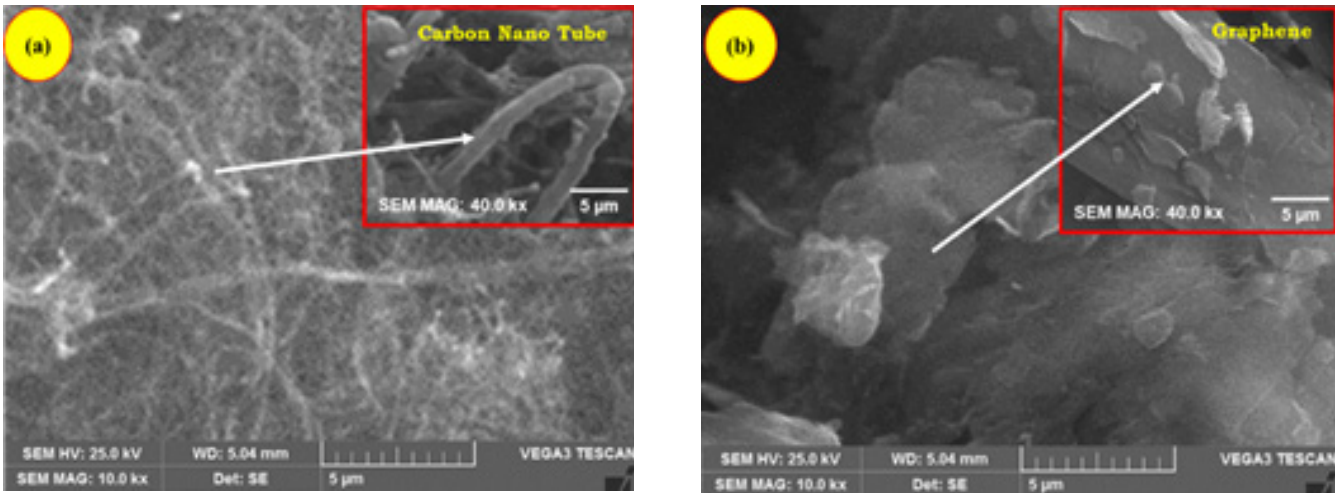

Figure 2. SEM micrographs of **(a)** CNT and **(b)** Graphene.

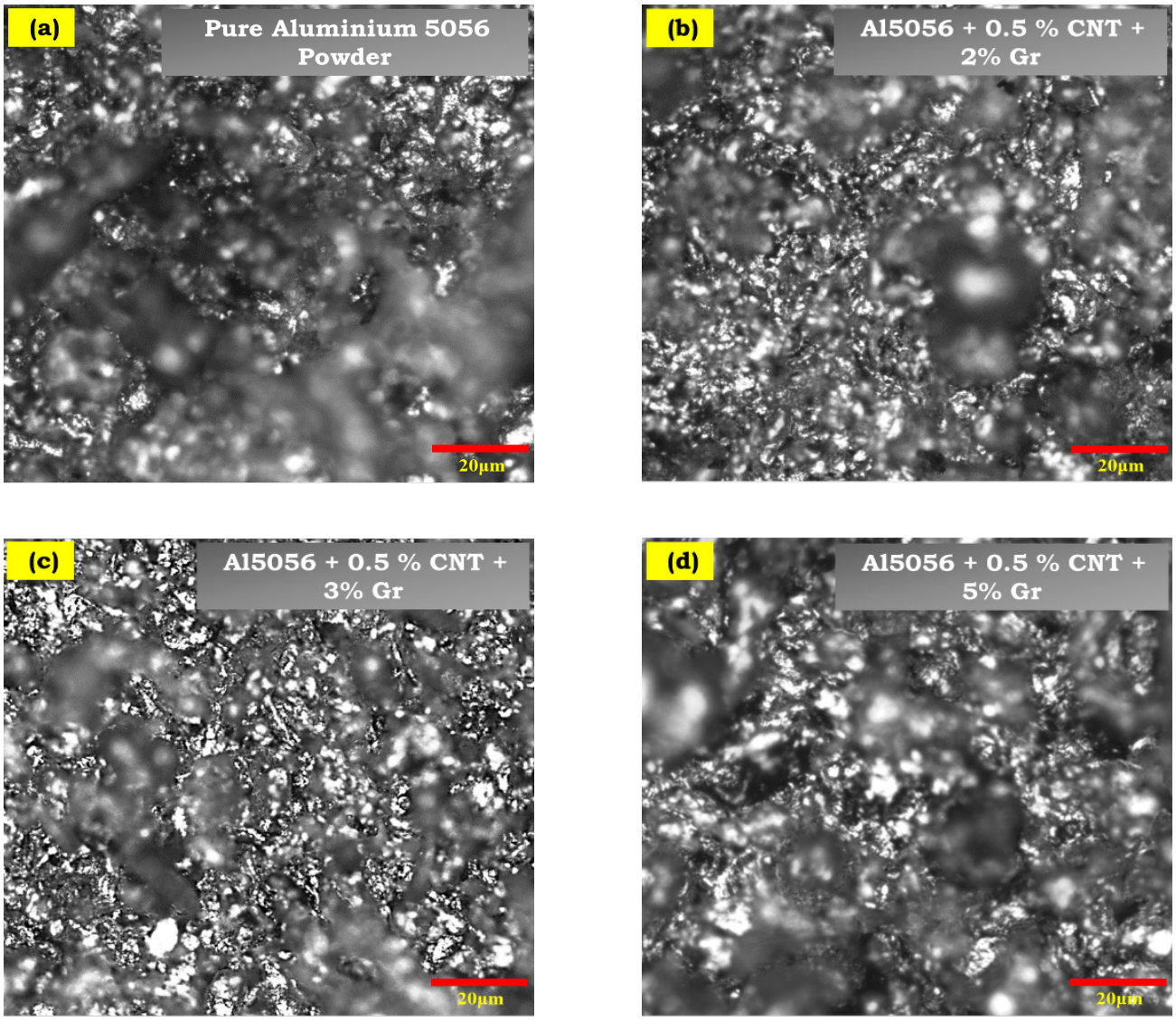

Figure 3. OM micrographs of Al 5056 alloy and its CNT/Gr hybrid- composites.

3.1.3 Hardness Test Results of Al5056 Alloy and its CNT/Gr Hybrid-Composites

From Figure 4 solidity surge with the upsurge in keeping Carbon Nanotube (CNT) continual and Graphene (Gr), we were gratified in the factual. Related to pure Al5056 alloy, 0.5% CNT + 2%Gr: Al5056-0.5C-2G adding displays a surge in 4.85 HV (5.74%), 0.5% CNT + 3%Gr: Al5056-0.5C-3G shows an increase in 11.96 HV (14.16%) respectively and further addition of 0.5% CNT + 5%Gr: Al5056-0.5C-5G shows an slight dip in the hardness value of 11.18 HV (13.24%) respectively The elevation in composition perchance be ascribed to unvarying dispersal

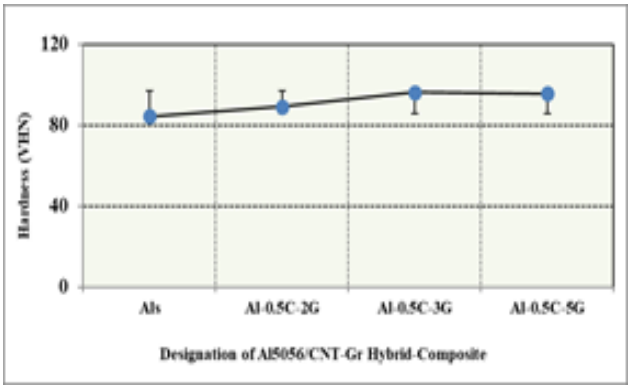

Figure 4. Hardness values of Al5056 alloy and its CNT/Gr hybrid-composites.

of buttressing (CNT and Gr) in the milieu material. From the figure, we can see a linear increment in hardness for Al-0.5C-2G and up to Al-0.5C-3G. Later as graphene is further increased to (5%) i.e., Al-0.5C-5G we can see the reduction compared to 3% Gr in the matrix because of agglomeration due to the addition of more buttressing milieu. This is due to the capacity stentorian ability of the bolstering in the milieu material[14,15].

3.1.4 *Tensile Test Results of Al5056 Alloy and its CNT/Gr Hybrid-composites*

From Figure 6 solidity surge with the upsurge in keeping carbon nanotube (CNT) continual and Graphene (Gr), we were gratified in the factual. Related to pure Al5056 alloy, 0.5% CNT + 2%Gr: Al5056-0.5C-2G adding displays an surge in 8.92 MPa (7.67%), 0.5% CNT + 3%Gr: Al5056-0.5C-3G shows an increase in 16.24

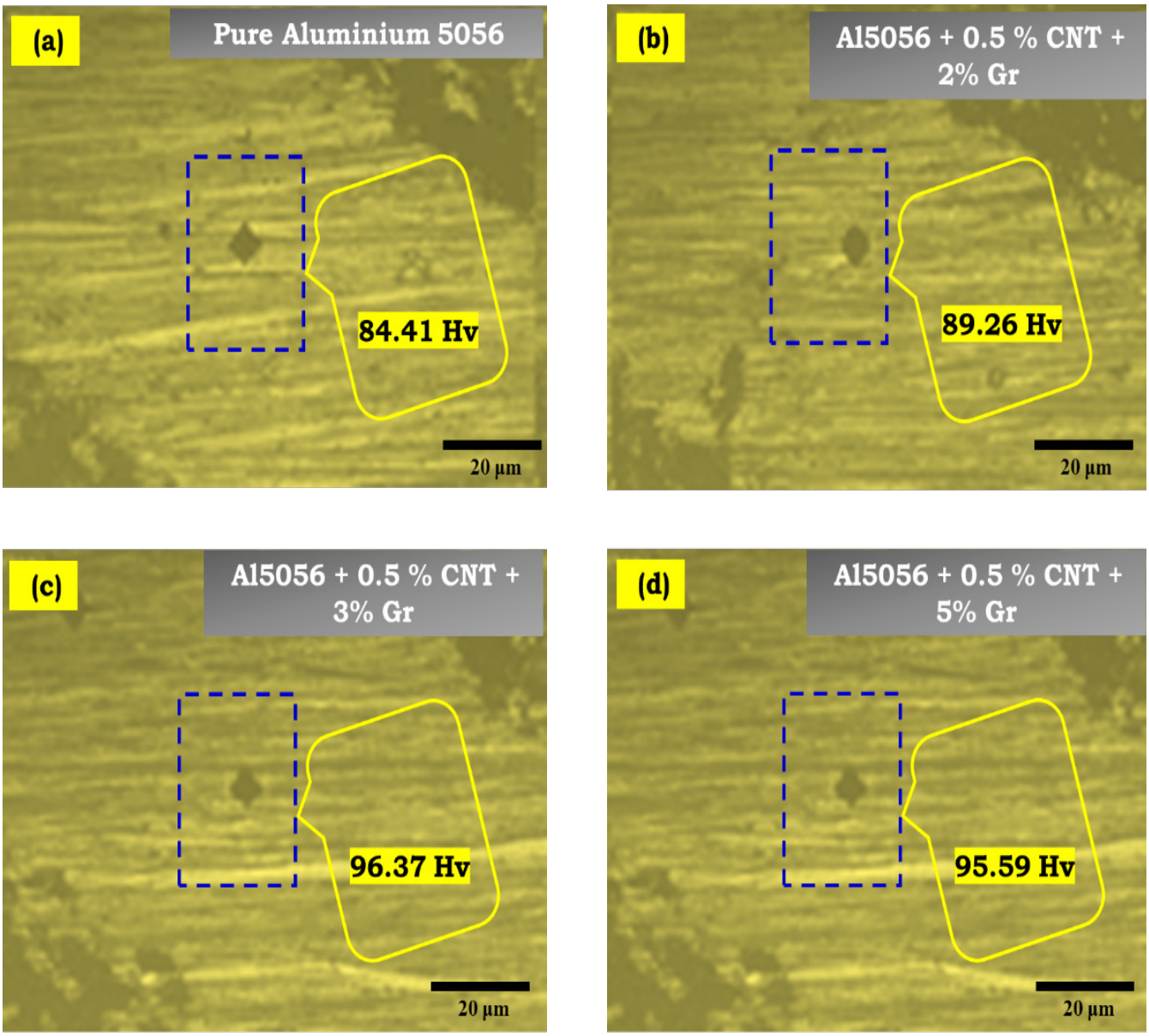

Figure 5. Hardness Indentation Result values of Al5056 alloy and its CNT/Gr hybrid-composites.

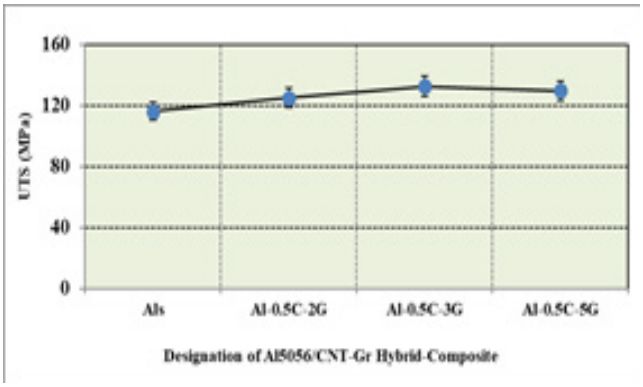

Figure 6. Tensile Strength (UTS) values Al5056 alloy and its CNT/Gr hybrid-composites.

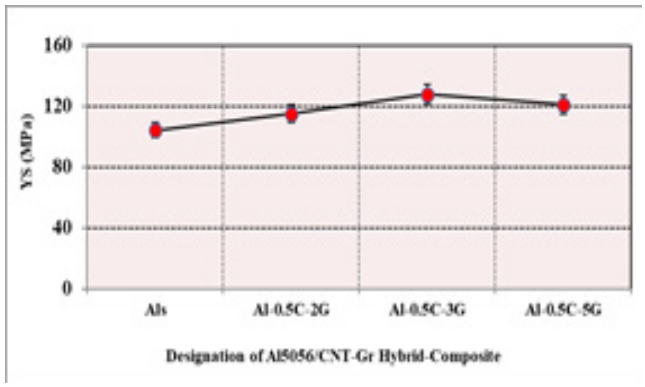

Figure 7. Tensile Strength (YS) values Al5056 alloy and its CNT/Gr hybrid-composites.

MPa (13.97%) respectively and further addition of 0.5% CNT + 5%Gr: Al5056-0.5C-5G shows an slight dip in the ultimate strength value of 13.47 MPa (11.59%) respectively The elevation in composition perchance be ascribed to unvarying dispersal of buttressing (CNT and Gr) in the milieu material. From the figure, we can see a linear increment in strength (TS) for Al-0.5C-2G and up to Al-0.5C-3G. Later as graphene is further increased to (5%) i.e., Al-0.5C-5G we can see the reduction compared to 3% Gr in the matrix because of agglomeration due to the addition of more buttressing milieu. This is due to the capacity stentorian ability of the bolstering in the milieu material[16-19].

From Figure 7 solidity surges with the upsurge in keeping Carbon Nanotube (CNT) continual and Graphene (Gr) gratified in the factual. Related to pure Al5056 alloy, 0.5% CNT + 2%Gr: Al5056-0.5C-2G adding displays a surge in 10.73 MPa (10.28%), 0.5% CNT + 3%Gr: Al5056-0.5C-3G shows an increase in 23.39 MPa (22.41%) respectively and further addition of 0.5% CNT + 5%Gr: Al5056-0.5C-5G shows an slight dip in the yield strength value of 16.83 MPa (16.12%) respectively the elevation in composition perchance be ascribed to unvarying dispersal of buttressing (CNT and Gr) in the milieu material. From the figure, we can see a linear increment in yield strength for Al-0.5C-2G and up to Al-0.5C-3G. Later graphene is further increased to (5%) i.e., Al-0.5C-5G.

We can see the reduction compared to 3% Gr in the matrix because of agglomeration due to the addition of a more buttressing milieu. This is due to the capacity stentorian ability of the bolstering in the milieu material[20-22].

3.1.5 Stress-Strain Curve (σ V/s ϵ) of Al5056 Alloy and its CNT/Gr Hybrid-composites

Figure 8 shows the stress and strain curves of Al5056 alloy and its CNT/Gr hybrid composites. From the 8 **(a)** depicts Al5056 alloy σ V/s ϵ curve, 8 **(b)** depicts σ V/s ϵ curve of Al5056 + (0.5% CNT + 2%Gr: Al-0.5C-2G) 8 **(c)** depicts σ V/s ϵ curve of Al5056 + (0.5% CNT + 3%Gr: Al-0.5C-3G) and 8 **(d)** depicts σ V/s ϵ curve of Al5056 + (0.5% CNT + 5%Gr: Al-0.5C-5G) its hybrid-composites.

Figure 9 shows the ductility values of Al5056 alloy and its CNT/Gr hybrid composites. The solidity surges with a decrease in keeping carbon nanotube (CNT) continual and Graphene (Gr) gratified in the factual. Related to pure Al5056 alloy, 0.5% CNT + 2%Gr: Al5056-0.5C-2G adding displays an abridged in 0.42 times (6.58%), 0.5%

CNT + 3%Gr: Al5056-0.5C-3G shows an abridged in 0.53 times (8.30%) respectively and further addition of 0.5% CNT + 5%Gr: Al5056-0.5C-5G shows a slight dip in the ductility value of 0.96 times (15.04%) respectively the elevation in composition perchance be ascribed to unvarying dispersal of buttressing (CNT and Gr) in the milieu material. From the figure, we can see a linear increment in ductility for Al5056-0.5C-2G and up to Al5056-0.5C-3G. Later as graphene is further increased to (5%) i.e., Al5056-0.5C-5G we can see the reduction compared to 3% Gr in matrix because of agglomeration due to the addition of more buttressing milieu. This is due to the capacity stentorian ability of the bolstering in the milieu material[23-25].

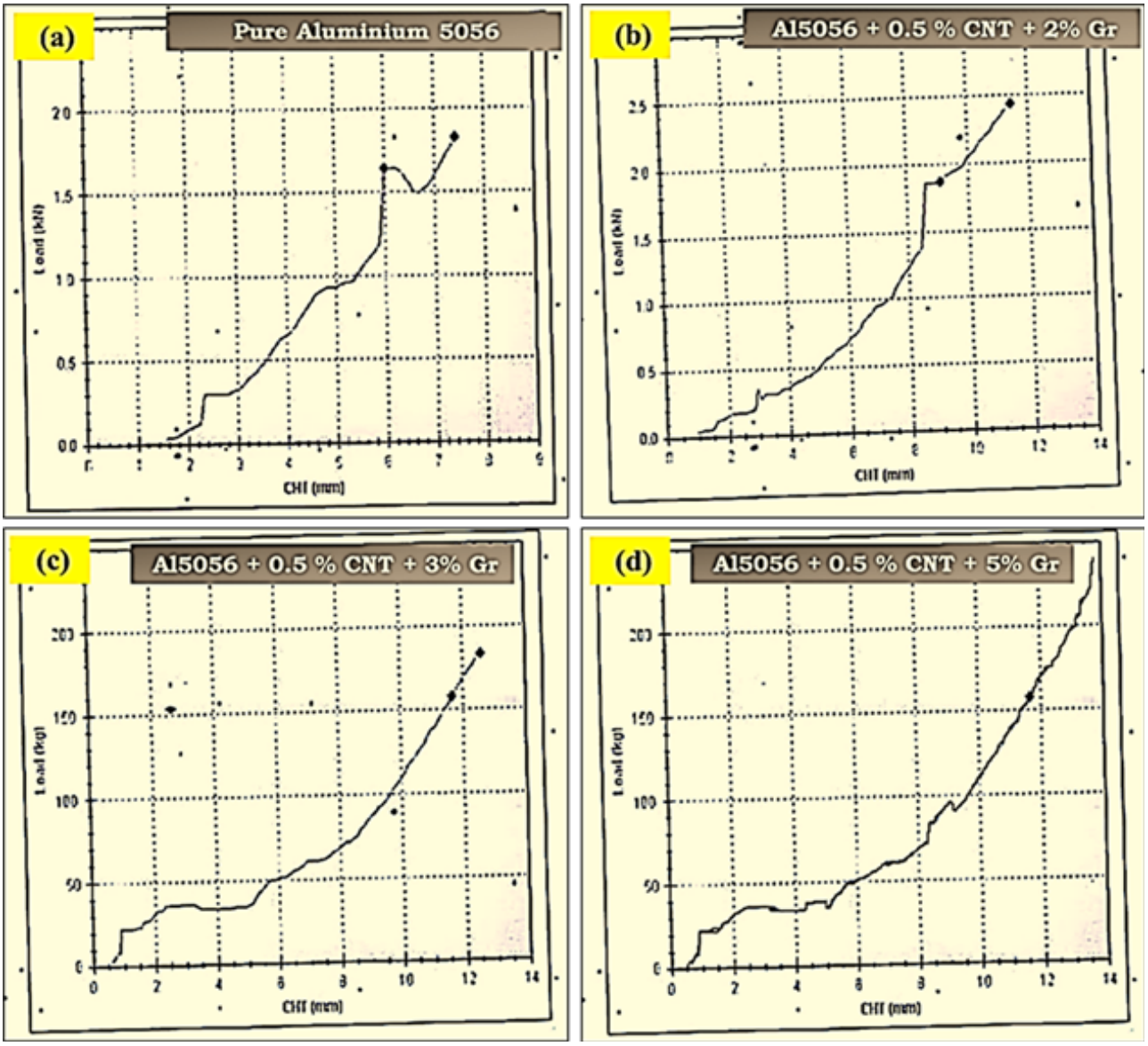

Figure 8. σ V/s ϵ curve of Al + (0.5% CNT + 5%Gr: Al-0.5C-5G).

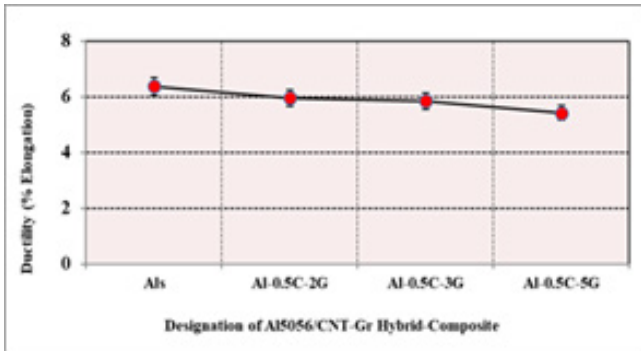

Figure 9. Ductility (% Elongation) values of Al5056 alloy and its CNT/Gr hybrid-composites.

3.1.6 Fractography Images of Al5056 Alloy and its CNT/Gr Hybrid-composites

Figure 10 shows a fractography analysis of Al5056 alloy and its CNT/Gr hybrid composites. From 10 (a) depicts Al alloy fractography analysis, 10 (b) depicts fractography analysis of Al5056 + (0.5% CNT + 2%Gr: Al-0.5C-2G) 10 (c) depicts fractography analysis of Al5056 + (0.5% CNT + 3%Gr: Al-0.5C-3G) and 10 (d) depicts fractography analysis of Al5056 + (0.5% CNT + 5%Gr: Al-0.5C-5G) its hybrid-composites. When the reinforcements square measure additional, the particulate cavalries type

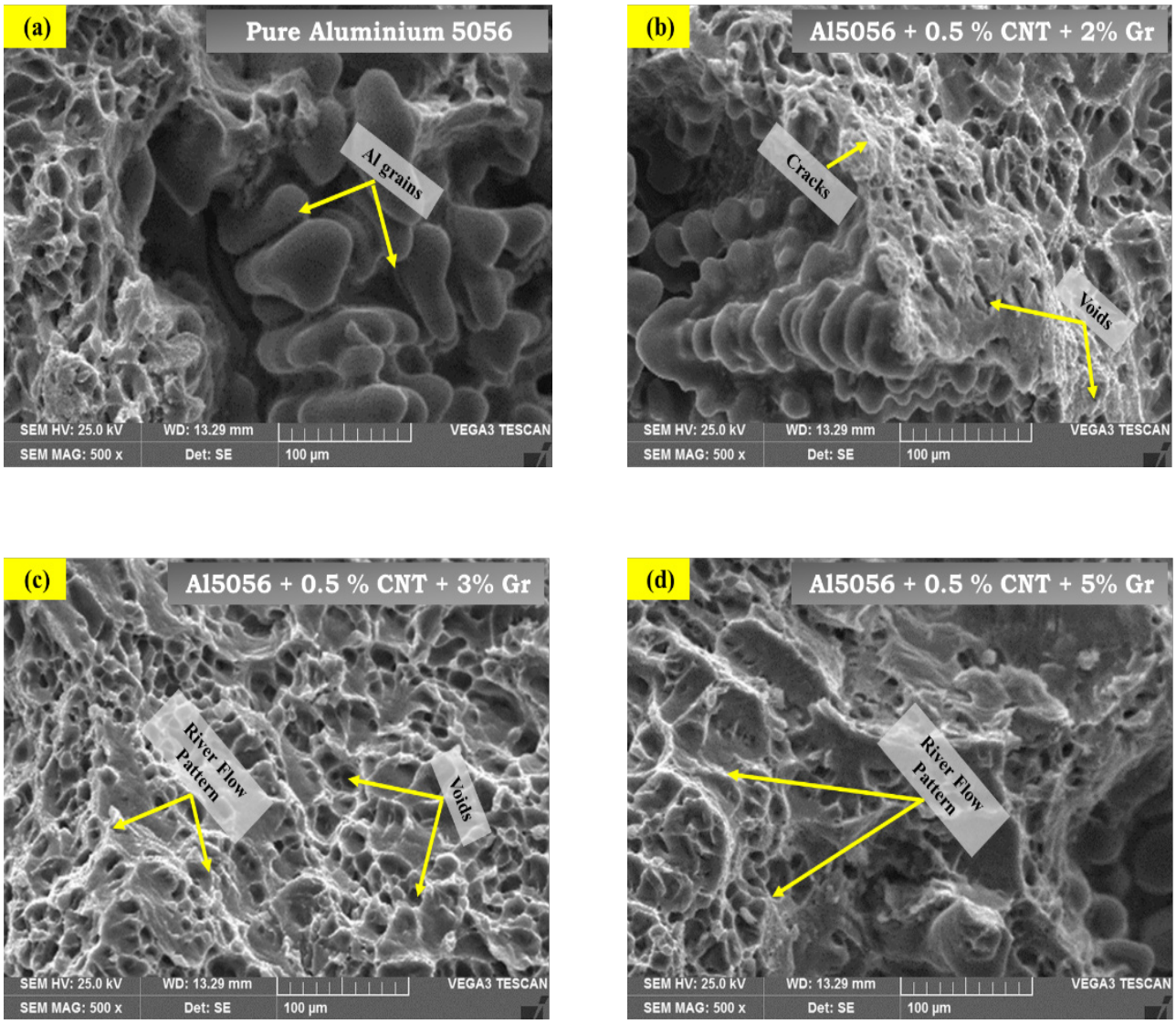

Figure 10. Fractography Analysis of Al5056 alloy and its CNT/Gr hybrid-composites.

nuclei end in the bigger numeral of smidgen formation. Therefore, the movement is restricted additional, which ends in bigger strength. Therefore, the observation within the overall increase of the lastingness is competent even and interpretable. The SEM micrographs of the fracture surfaces of the tensile take a look at specimen square measure shows that the fracture may be expected from ductile fracture in Al alloy and brittle fracture in Al/CNT/Gr hybrid-composites. From the 10 (a) in the SEM Fractographs of Al alloy we can see bulky size dints indicative of the fracture of pure alloy by pliable fracture. From the 10 (b) in the SEM Fractographs of Al + (0.5% CNT + 2%Gr: Al-0.5C-2G), we can see bulky size dints with lesser size dints indicative of the fracture of Al-0.5C-2G by frail fracture. From the 10 (c) in the SEM Fractographs of Al + (0.5% CNT + 3%Gr: Al-0.5C-3G), we can see bulky size dints with lesser size dints indicative of the fracture of Al-0.5C-3G by fragile fracture. From the 10 (d) in the SEM Fractographs of Al + (0.5% CNT + 5%Gr: Al-0.5C-5G), we can see bulky size dints with lesser size dints indicative of the fracture of Al-0.5C-5G by brittle fracture[26].

3.1.7 *Wear Test Results of Al5056 Alloy and its CNT/Gr Hybrid-Composites*

Figure 11 displays the wear rate of Al5056 alloy and its CNT/Gr hybrid composites. It can be noted that as the load rises the wear rate improves. Also, we can see that up to a load of 20N wear increases and there is a slight dip and again there is a steep rise in the curve for a load of 40N and increases further at a load of 50N. So, we can observe that the lowest wear is for a load of 10N for Al alloy (i.e., 1.5312 mm^3/m) and peak wear is for a load of 50N (i.e., 1.5342 mm^3/m). Likewise, for 0.5% CNT + 2%Gr: Al5056-0.5C-2G lowest wear is for a load of 10N (i.e., 1.4381 mm^3/m) and peak wear is for a load of 50N (i.e., 1.4548 mm^3/m). Also, for 0.5% CNT + 3%Gr: Al5056-0.5C-3G lowest wear is for a load of 10N (i.e., 1.4311 mm^3/m) and peak wear is for a load of 50N (i.e., 1.4572 mm^3/m). Similarly, for 0.5% CNT + 5%Gr: Al5056-0.5C-5G lowest wear is for a load of 10N (i.e., 1.4247 mm^3/m) and peak wear is for a load of 50N (i.e., 1.4515 mm^3/m). One thing is observed i.e., hybrid-MMC has a lower wear rate than Al5056-alloy. This is because of the shielding influence of CNT and Gr in the Al-matrix. Related outcomes were noted by a few investigators[27,28].

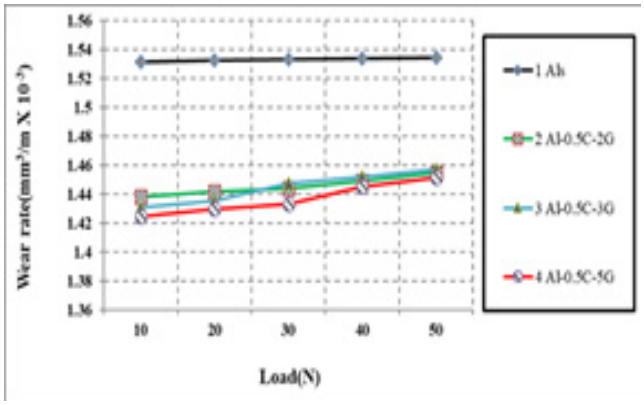

Figure 9. Ductility (% Elongation) values of Al5056 alloy and its CNT/Gr hybrid-composites.

3.1.8 *Wear Track Study of Al5056 Alloy and its CNT/Gr Hybrid-Composites*

Figure 12 shows the WSM Al5056 alloy and its CNT/Gr hybrid composites. Where 12 (a)WSM of Al5056 matrix alloy, 12 (b) WSM of Al5056 matrix alloy + 0.5% CNT + 2% Gr: Al5056-0.5C-2G, 12 (c) WSM of Al5056 matrix alloy + 0.5% CNT + 3%Gr: Al5056-0.5C-3G, 12 (d) WSM of Al matrix alloy + 0.5% CNT + 5%Gr: Al5056-0.5C-5G. WSM is taken at a Parameter of Load: 50N, Slithering Velocity: 2.0 m/sec, Slithering Distance: 1000 meters. The wear development occurring here concerned the brim formation and material removal materialized by plastic deformation thanks to a high load of 50N. The wear and tear surface morphology of Al5056 alloy is suave with fewer cracks. The examination of the wear surfaces of the Al and the different wt. % of CNT and Gr hybrid-composites at higher magnification reveals discrete configuration of trenches seriatim parallel to one another in the slithering direction witnessed in Figure 12 (b-d). Related outcomes were noted by a few investigators[29,30].

4. Conclusion

Since examinations were done in a bid to verify the mechanical properties of CNT/Gr reinforced Al 5056 composites of distinct Wt % of the fortification, it has been noticed that:

(i) SEM Micrographs of elegant samples, the subsequent stayed examined:

- The distribution of reinforcement particles (CNT/Gr) is found to be uniform.
- The CNT/Gr particles are not trapped in the grain boundaries.
- The margin of CNT/Gr fragments are sited within the matrix which implies improved drenched expected by adding Mg as a soaking agent.
- The CNT/Gr Flakes gets initiation of great soaking through the matrix as it is beneficial in the upsurge of mechanical properties.

(ii) CNT/Gr Flakes as corroboration aided in upsurging the hardness (VHN) of Al5056 CNT/Gr hybrid composites to about 11.04 % contrasted to that of the Al5056 alloy.

(iii) CNT/Gr Flakes as corroboration abetted in increasing the tensile strength (UTS) of Al5056 CNT/Gr hybrid composites to about 11.07% contrasted to that of the Al5056 alloy.

(iv) CNT/Gr Flakes as corroboration abetted in increasing the Tensile strength (YS) of Al5056 CNT/Gr hybrid composites to about 16.27% contrasted to that of the Al5056 alloy.

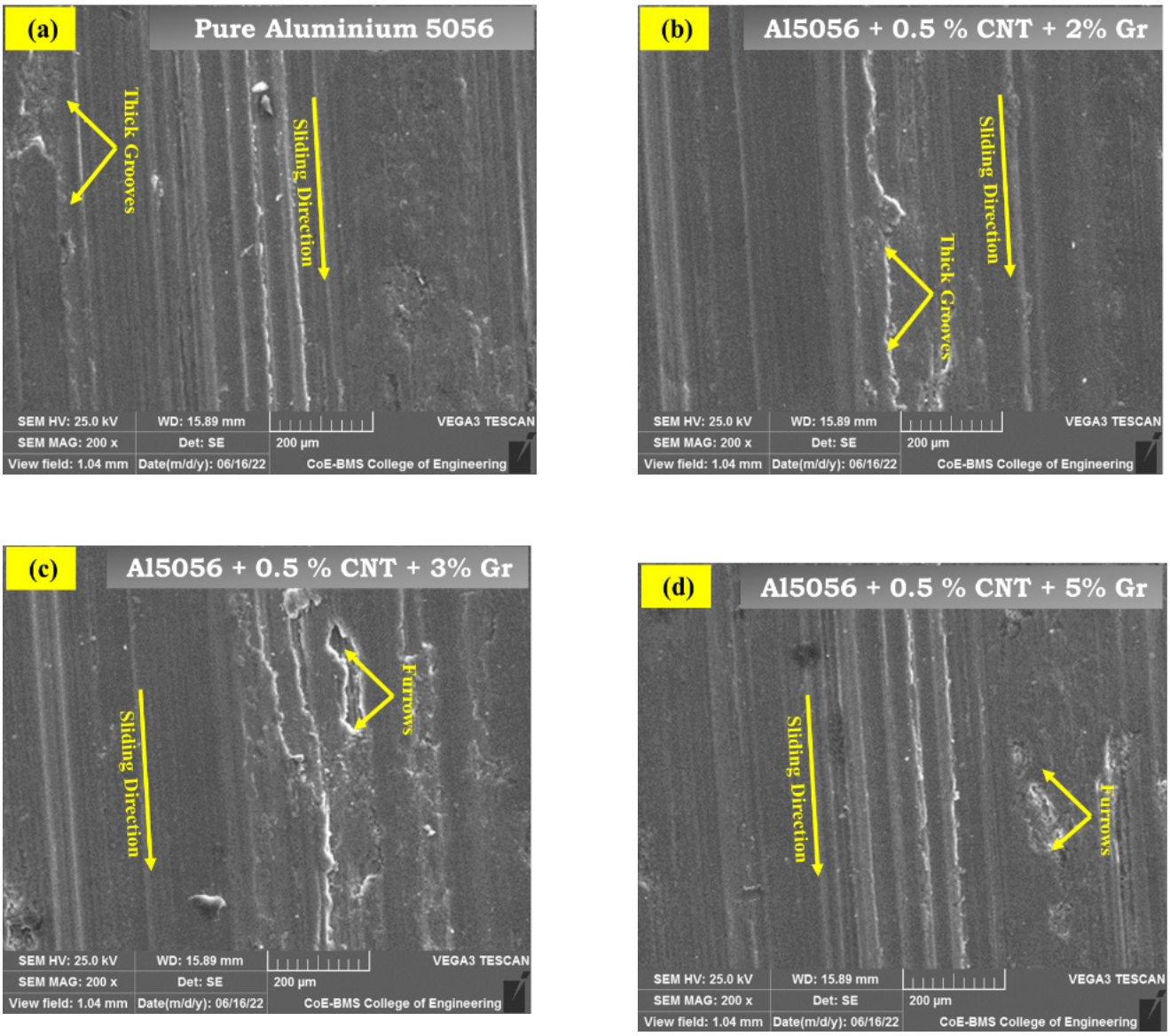

Figure 12. Wear surface analysis of Al5056 alloy and its CNT/Gr hybrid composites.

(v) CNT/Gr Flakes as corroboration abetted in reducing the Ductility (% Elongation) of Al5056 CNT/Gr hybrid composites to about 9.97% contrasted to that of the Al5056 alloy.

(vi) Wear tracks of Al5056 alloy reveal a tough face with more trenches and ridges assessed to wear tracks of Al5056/CNT-Gr hybrid composites.

5. References

1. Girish BM, Siddesh HS, Satish BM. Taguchi grey relational analysis for parametric optimization of severe plastic deformation process. SN Applied Sciences. 2019; 1 (8), 1-11. https://doi.org/10.1007/s42452-019-0982-6
2. Sharma SC, Girish BM, Satish BM, Kamath R. Ageing characteristics of short glass fibre reinforced ZA-27 alloy composite materials. Journal of Materials Engineering and Performance. 1998; 7(6):747-50. https://doi.org/10.1361/105994998770347305
3. Avinash L, Angadi S, Malik V, Saxena KK, Prakash C, Dixit S, Mohammed KA. Mechanical and tribological properties of aluminium-based metal-matrix composites. Materials. 2022; 15:6111. https://doi.org/10.3390/ma15176111 PMid:36079492 PMCid: PMC9458116

4. Lakshmikanthan A, Ramprabhu T, Udayagiri SB, Koppad PG, Gupta M, Munishamaiah K, Bontha S. The effect of heat treatment on the mechanical and tribological properties of dual size SiC reinforced A357 matrix composites. Journal of Materials Research and Technology. 2020; 9(3):6434-52. https://doi.org/10.1016/j.jmrt.2020.04.027
5. Lakshmikanthan A, Bontha S, Krishna M, Koppad PG, Ramprabhu T. Microstructure, mechanical and wear properties of the A357 composites reinforced with dual-sized SiC particles. Journal of Alloys and Compounds. 2019; 786(25):570-80. https://doi.org/10.1016/j.jallcom.2019.01.382
6. Vani VV, Chak SK. The effect of process parameters in aluminium metal matrix composites with powder metallurgy. Manuf Rev. 5, 2018. https://doi.org/10.1051/mfreview/2018001
7. Sharma AK, Bhandari R, Aherwar A, Rimašauskienė R, Pinca-Bretotean. A study of advancement in application opportunities of Aluminium metal matrix composites. Mater Today Proc. 2020; 26(2):2419-24. https://doi.org/10.1016/j.matpr.2020.02.516
8. Kumar SV, Prasad MG, Avinash L, Praveen BA, Singh Yadav SP, Chacko A. Prediction of thermal conductivity for Al6061 reinforced with silicon carbide and graphite using statistical approach. In: Narendranth S, Mukunda PG, Saha, UK, editors. Recent advances in mechanical engineering. Lecture Notes in Mechanical Engineering. Singapore: Springer; 2023. https://doi.org/10.1007/978-981-19-1388-4_18
9. Marwaha R, Gupta RD, *et al*. Determination and experimental investigation of weight loss on Al/SiC/Gr-Metal matrix hybrid composite by Taguchi method. Int J Sci Eng Technol. 2013; 2:2038-48.
10. Jamwal A, Vates UK, Gupta P, Aggarwal A, Sharma BP. Fabrication, and characterization of Al_2O_3– TiC reinforced Aluminium matrix composites. Advances in industrial and production engineering. Singapore: Springer; 2019. p. 349–56. https://doi.org/10.1007/978-981-13-6412-9_33
11. Kumar R, Pridhar K, Balaji S. Mechanical properties and characterization of Zirconium Oxide (ZrO_2) and Coconut Shell Ash (CSA) reinforced Aluminium (Al 6082) matrix hybrid composite. Journal of Alloys and Compounds. 2018; 765:171–9. https://doi.org/10.1016/j.jallcom.2018.06.177
12. Gnanavelbabu A, Arunachalam V, Surendran KTS, Rajkumar K. Optimization of machining parameters in CNC turning of AA6061-B_4C-CNT hybrid composites using the grey-fuzzy method. IOP Conference Series: Materials Science and Engineering. 2020; 764(1):012010. https://doi.org/10.1088/1757-899X/764/1/012010
13. Madgule M, Sreenivasa CG, Patel CGM, Avinash L, Singhal P, Pandit D, Malik V. Influence of foaming agents on mechanical and microstructure characterization of AA6061 metal foams. Proc IMechE Part E: J Process Mechanical Engineering. 2022; 1-13. https://doi.org/10.1177/09544089221097534
14. Yang L, Pu B, Zhang X, Sha J, He C, Zhao N. Manipulating mechanical properties of graphene/Al composites by an *in-situ* synthesized hybrid reinforcement strategy. Journal of Materials Science and Technology. 2022; 123:13–25. https://doi.org/10.1016/j.jmst.2021.12.072
15. Wang X, Su Y, Qiu C, *et al.* Mechanical behaviour and interfacial micro-zones of SiCp (CNT) hybrid reinforced aluminium matrix composites. Materials Characterization. 189; 111982. https://doi.org/10.1016/j.matchar.2022.111982
16. Thiyaneshwaran N, Selvan CP, Avinash L, Sivaprasad K, Ravisankar B. Comparison based on specific strength and density of *in-situ* Ti/Al and Ti/Ni metal intermetallic laminates. Journal of Materials Research and Technology-Elsevier. 2021; 14:1126-36. https://doi.org/10.1016/j.jmrt.2021.06.102
17. Li Q, Zhang GD, Blucher JT, Cornie JA. Microstructure of the interface and interfiber regions in P-55 reinforced aluminium alloys manufactured by pressure infiltration. In Proceedings of the 3rd International Conference on Composite Interfaces (ICCI-III), Cleveland, OH, USA; 1990.
18. Siqueira ML, Aline da Silva, *et al.* Mechanical properties analysis of Al2024 alloy submitted to different ageing time different cold plastic deformation degree. Mater Res. 2019; 22. https://doi.org/10.1590/1980-5373-mr-2018-0598
19. Santosh J, Zhai SP, Chen Y, Zhao J, Huang Z. Hierarchical toughening of laminated nanocomposites with three-dimensional graphene/carbon nanotube/SiC nanowire. Materials Today Nano. 2022; 18:100180. https://doi.org/10.1016/j.mtnano.2022.100180
20. Chate GR, Kulkarni RM, Chandrashekarappa MPG, Avinash L, Harsha HM, Tophakhane S, Shaikh N, Kongi S, Iranava P. Synthesis and characterization of Fe_2O_3 nanoparticles reinforced to recycled industrial aluminium scrap and waste aluminium beverage cans for preparing metal matrix nanocomposites. Frattura ed Integrità strutturale. 2022; 16(60): 229-42. https://doi.org/10.3221/IGF-ESIS.60.16

21. Moustafa EB, Melaibari A, Alsoruji G, Khalil AM, Mosleh AO. The tribological and mechanical characteristics of AA5083 alloy are reinforced by hybridising heavy ceramic particles Ta_2C and VC with light GNP and Al_2O_3 nanoparticles. Ceramics International. 2022; 48(4):4710–21. https://doi.org/10.1016/j.ceramint.2021.11.007
22. Naik HRM, Manjunath LH, Vinayak R, Manjunath GC, Kuldeep K, Avinash L. Effect of microstructure, mechanical and wear on Al-CNTs/Graphene hybrid MMCs. Advances in Materials-and-Processing Technologies. 2021; 8:2,366-79. https://doi.org/10.1080/2374068X.2021.1927646
23. Riaz H, Manzoor T, Raza A. Fabrication and characterization of AA6061/CNTs surface nanocomposite by friction stir processing. International Journal of Advanced Manufacturing Technology. 2019; 105(1–4):749–69. https://doi.org/10.1007/s00170-019-04243-7
24. Lakshmikanthan A, Mahesh V, Prabhu RT, Patel MGC, Bontha S. Free vibration analysis of A357 alloy reinforced with dual particle size silicon carbide metal matrix composite plates using finite element method. Archives of Foundry Engineering. 2021; 21(1):101–12. https://doi.org/10.24425/afe.2021.136085
25. Naik MHR, Manjunath LH, Vishwanath K, Avinash L, Koppad PG, Kumaran SP. Al/Graphene/CNT hybrid composites: Hardness and sliding wear studies. FME Transactions. 2021; 49:414-21. https://doi.org/10.5937/fme2102414N
26. Muniyappan M, Iyandurai N. Structural morphology, elemental composition, mechanical and tribological properties of the effect of carbon nanotubes and silicon nanoparticles on A.A. 2024 hybrid metal matrix composites. SAE International Journal of Materials and Manufacturing. 2022; 15(2):203. https://doi.org/10.4271/05-15-02-0013 PMid:28244547
27. Hatti G, Lakshmikanthan A, Naveen GJ. Microstructure characterization, mechanical and wear behaviour of silicon carbide and neem leaf powder reinforced AL7075 alloy hybrid MMCs. Frattura ed Integrità Strutturale. 2023; 65:88-99. https://doi.org/10.3221/IGF-ESIS.65.07
28. Kareem A, Qudeiri JA, Abdudeen A, Ahammed T, Ziout A. A review on aa 6061 metal matrix composites produced by stir casting. Materials. 2021; 14(1):175–222. https://doi.org/10.3390/ma14010175.PMid:33401426 PMCid: PMC7796217
29. Anwar J, Khan M, Farooq MU *et al.* Effect of B_4C and CNTs' nanoparticle reinforcement on the mechanical and corrosion properties in rolled Al 5083 friction stir welds. Canadian Metallurgical Quarterly. 2022; 1–10. https://doi.org/10.1080/00084433.2022.2054586
30. Suthar J, Patel K. Corrosion behaviour of Mg, graphite-, B_4C and Ti-reinforced hybrid aluminium composites. Journal of The Institution of Engineers (India): Series C. 2022. https://doi.org/10.1007/s40032-021-00785-6
31. Carvalho O, Miranda G, Buciumeanu M, Gasik M, Silva FS, Madeira S. High temperature damping behaviour and dynamic Young's modulus of AlSi–CNT–SiCp hybrid composite. Composite Structures. 2016; 141:155–62. https://doi.org/10.1016/j.compstruct.2016.01.046